



iPOP 2005

Some Key Technologies on Future Optical IP Networks

G.S. Kuo, Xiaohua Ma, Qing Huang, Hai-Bo
Guo, Yong Yin, Yao Dong, Wei Qin, Xin Xie
and Ling Wang

Beijing University of Posts and Telecommunications
National Chengchi University

A decorative graphic consisting of a yellow square, a blue square, and a black crosshair.

Contents

- Control Plane in GMPLS-Based IP Networks
- Routing and Wavelength Assignment (RWA) in GMPLS-Based IP Networks
- Protection & Restoration in GMPLS-Based IP Networks
- Design of MOEMS-based GMPLS-oriented Optical Switching System

A decorative graphic on the left side of the slide, consisting of a yellow square, a blue square, and a black crosshair.

PART I

Control Plane in GMPLS-Based IP Networks

A decorative graphic on the left side of the slide, consisting of a yellow square, a blue square, and a black crosshair.

Research Results

- An Integrated Routing Protocol
- An Improved Fault Localization Scheme

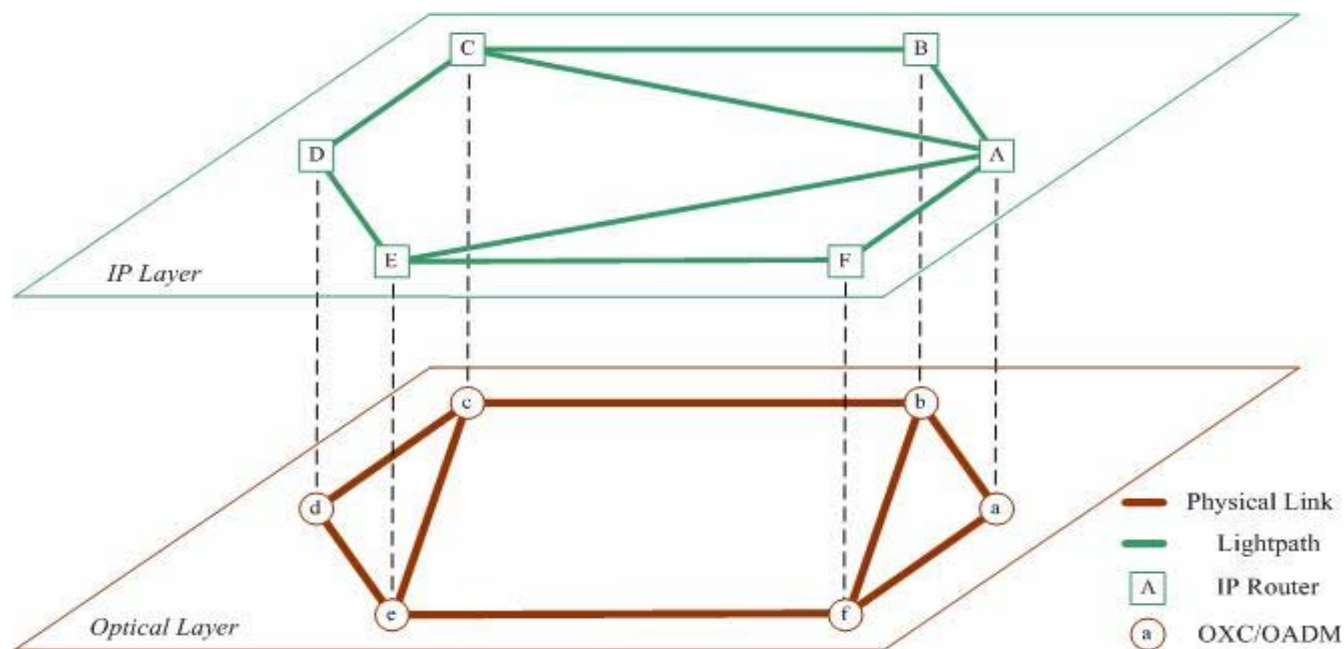


An Integrated Routing Protocol

- Traditionally, OSPF in IP layer and OSPF-TE in optical layer work independently. This mechanism is complex and its O&M cost is high. Furthermore, control overheads are very heavy.
- Our proposed routing protocol works for both layers simultaneously. Wavelength availability information is carried out. Its control overhead can be reduced from several to about ten times.

An Integrated Routing Protocol

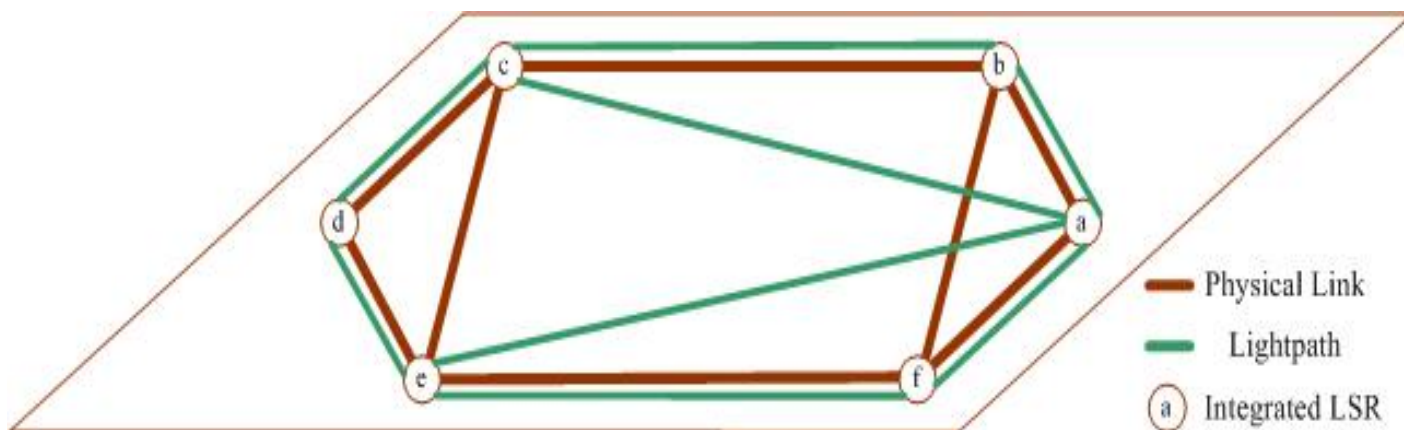
The Conventional OSPF/OSPF-TE



1. OSPF in IP layer and OSPF-TE in optical layer work independently.
2. The overheads of advertising Link State Advertisement (LSA) are very heavy.

An Integrated Routing Protocol

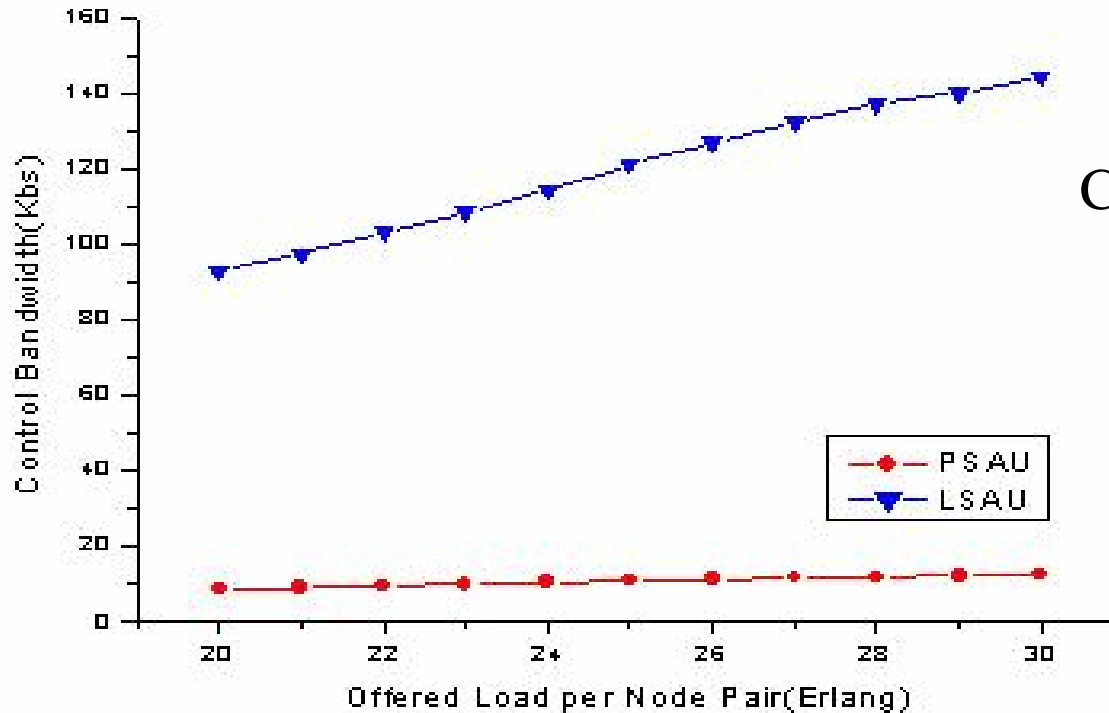
The Proposed Integrated OSPF-TE



1. OSPF-TE notifies how many bandwidths change (reserved or released) on all involved physical links.
2. Only source LSR floods LSAs.
3. LSAs are transmitted only on network's control channels.
LSAs are never transmitted on lightpaths (i.e., IP links).

An Integrated Routing Protocol

Simulation Results of Routing Protocols



Control overheads are reduced greatly.

LSAU: the conventional routing protocol

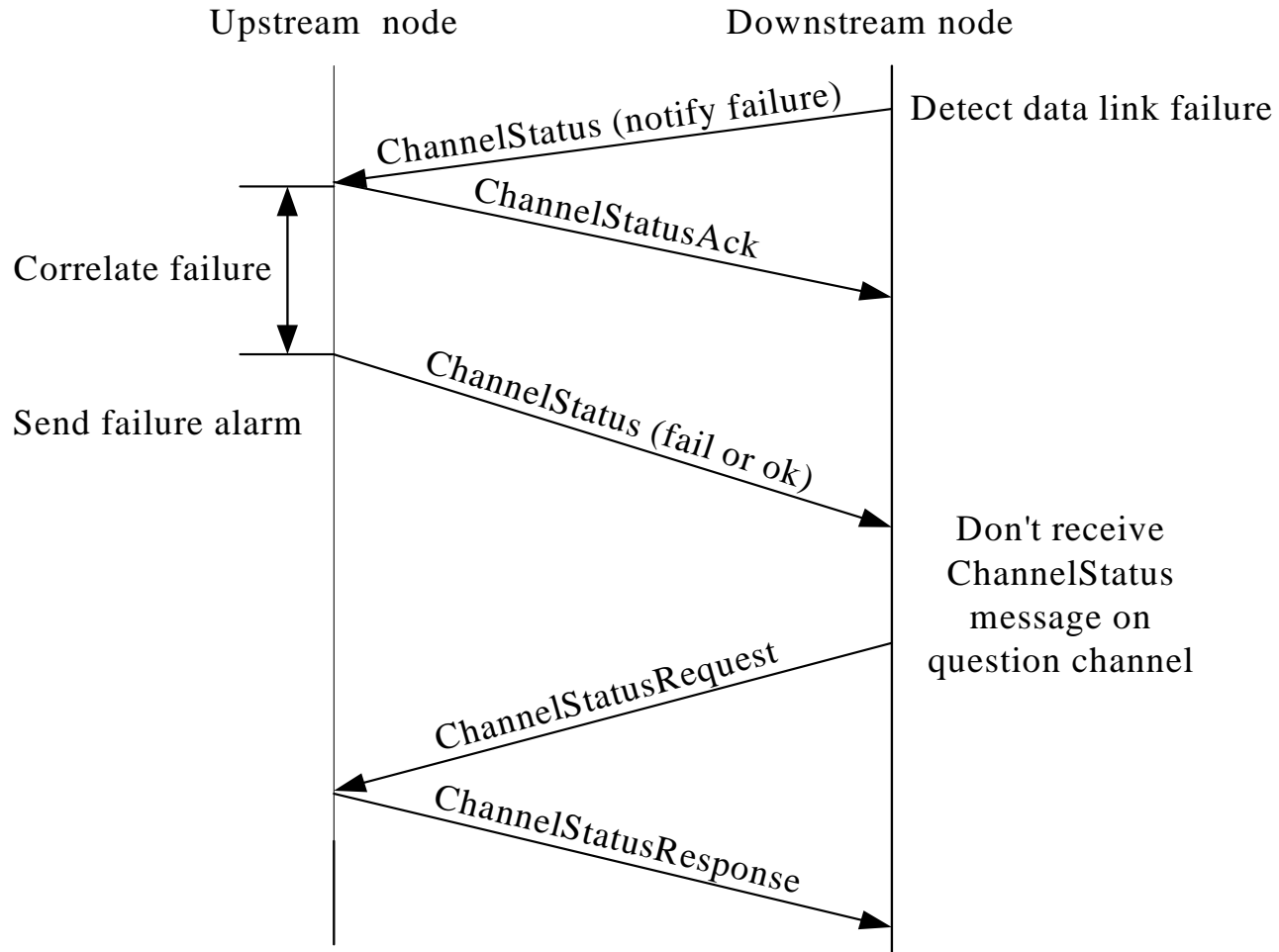
PSAU: the proposed routing protocol



An Improved Fault Localization Scheme

The Flaws behind Current Fault Localization Scheme

- Many unnecessary fault correlation procedures.
- There are many redundant messages in current fault localization procedure.



The fault localization procedure between two adjacent nodes in current LMP.



An Improved Fault Localization Scheme

The Proposed Scheme:

- A new fault localization procedure, which employs a bi-directional data link failure notification approach, as a substitute of current version.
- By employing our scheme, the data/TE link failure is quickly located with much lower signaling overhead and network resource occupancy.



An Improved Fault Localization Scheme

The Advantages of Proposed Scheme:

- The signaling overhead for locating a data link failure is remarkably reduced.
- The much lower network resource occupancy.
- The mistaken isolation of healthy links is avoided.



An Improved Fault Localization Scheme

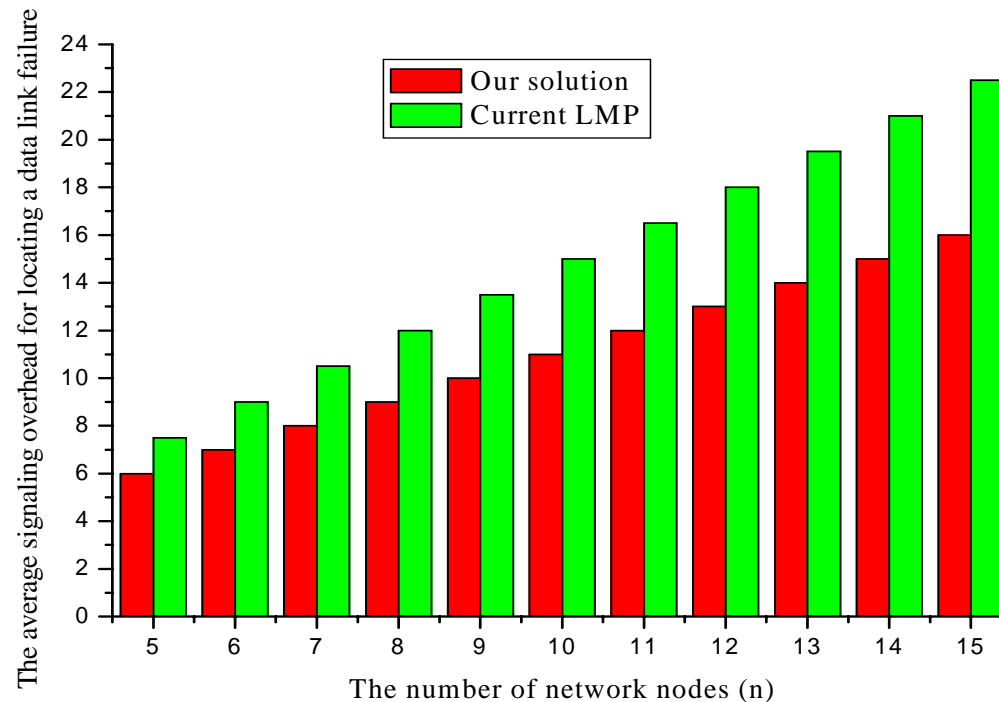
Performance Comparison

- The average signaling overhead in our solution, $E[N_{new}]$, and that in current version, $E[N_{old}]$, can be obtained respectively.

$$E[N_{new}] = \sum_{i=1}^{n-1} P_i N_{i-new} = \sum_{i=1}^{n-1} \frac{1}{n-1} \cdot [2(n-i) + 1]$$

$$E[N_{old}] = \sum_{i=1}^{n-1} P_i N_{i-old} = \sum_{i=1}^{n-1} \frac{1}{n-1} \cdot 3(n-i)$$

- For locating a failure, the average signaling overhead in proposed solution is always lower than that in current version. For example, when the number of network nodes is 10 and 15, the average signaling overhead in our solution is decreased 26.7% and 28.9% respectively.



The average signaling overhead for locating a data link failure, which affects one direction of a bi-directional TE link.

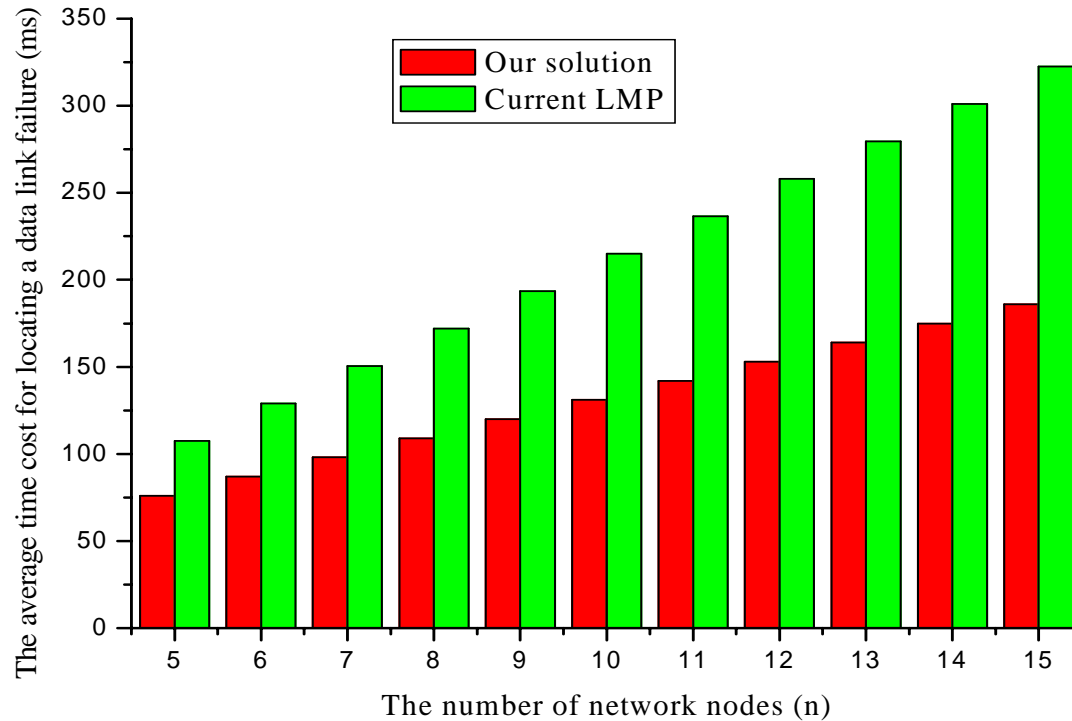
An Improved Fault Localization Scheme

For locating a data link failure, the average time cost in our scheme, $E[T_{new}]$, and that in current scheme, $E[T_{old}]$, can be computed as follows.

$$E[T_{new}] = \sum_{i=1}^{n-1} P_i T_{i-new} = \sum_{i=1}^{n-1} \frac{1}{n-1} \cdot \{ [2(n-i)+1] \cdot (T_{trans} + T_{proc}) + T_{correlate} \}$$

$$E[T_{old}] = \sum_{i=1}^{n-1} P_i T_{i-old} = \sum_{i=1}^{n-1} \frac{1}{n-1} \cdot [3(n-i) \cdot (T_{trans} + T_{proc}) + (n-i) \cdot T_{correlate}]$$

Compared with current scheme, the average time cost in our scheme is decreased 39.1% (n=10) and 42.3% (n=15) respectively.



The average time cost for locating a data link failure, which affects one direction of a bi-directional TE link.



PART II

Routing and Wavelength Assignment (RWA) in GMPLS-Based IP Networks



Research Motivation

- Before a lightpath is set up, a route must be selected and a wavelength must be assigned.
- A suitable RWA algorithm can reduce blocking probability and increase network utilization efficiency.



Research Goal

- To propose a mathematical model to analyze the blocking probability in wavelength-routed networks.
- To propose a method to improve fairness between longer-hop connections and short-hop connections.



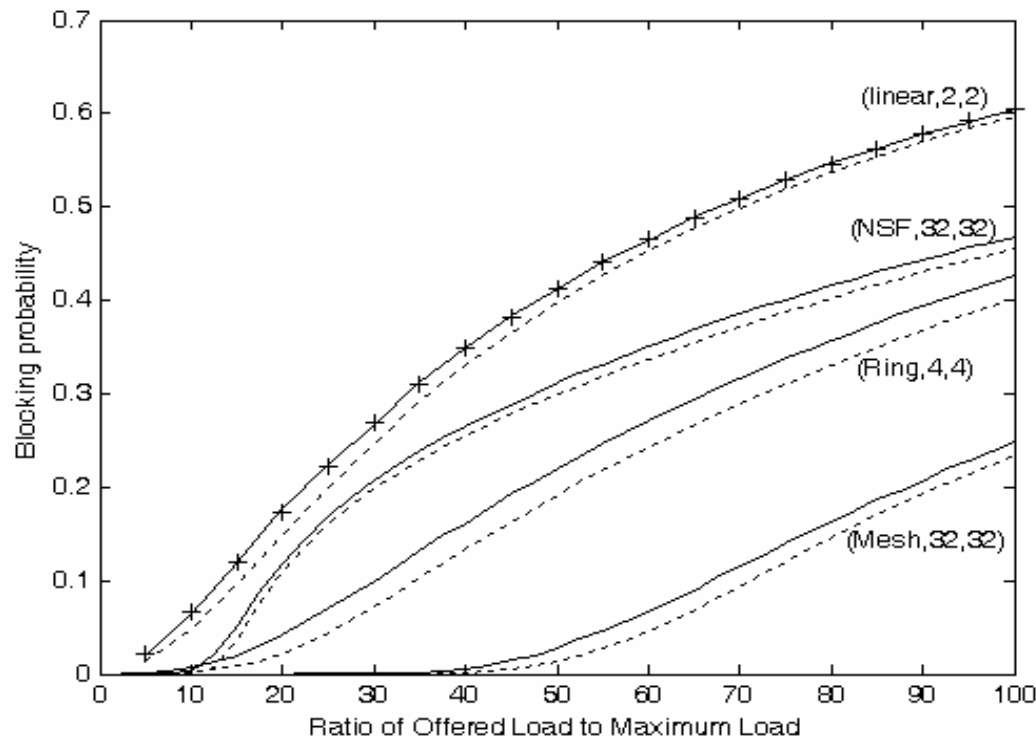
Research Results (I)

A Novel Blocking Analysis Method in Wavelength-Routed Networks

- The computational complexities of analyzing blocking probability in conventional ways grow exponentially with the number of wavelengths, W .
- The proposed method's computational complexity is independent of W .

Research Results (I)

A Novel Blocking Analysis Method in Wavelength-Routed Networks



- Solid line: the simulation results
- Dotted line: the proposed method's results
- Plus sign: the accurate analytical results



Research Results (II)

Fairness Improvements in GMPLS-based Wavelength-Routed Networks

- It improves the fairness.
- The performance of shorter-hop connections is not degraded much.
- The network utilization is increased as much as possible.

A decorative graphic on the left side of the slide, consisting of a yellow square, a blue square, and a black crosshair.

PART III

Protection & Restoration in GMPLS-Based IP Networks



Research Motivation (I)

- Due to the explosive growth of real-time and multimedia-oriented services on Internet, network survivability becomes much more important than before.
- Even a small failure of link or node is unacceptable.
- Protection and Restoration (P&R) are the important techniques to improve network survivability.



Research Motivation (II)

- Many P&R mechanisms have been developed in GMPLS-based networks.
- These mechanisms do not solve the issues such as shared mesh restoration, time guarantee recovery, etc.
- Some mechanisms are impractical to be implemented due to high complexity.



Research Goal

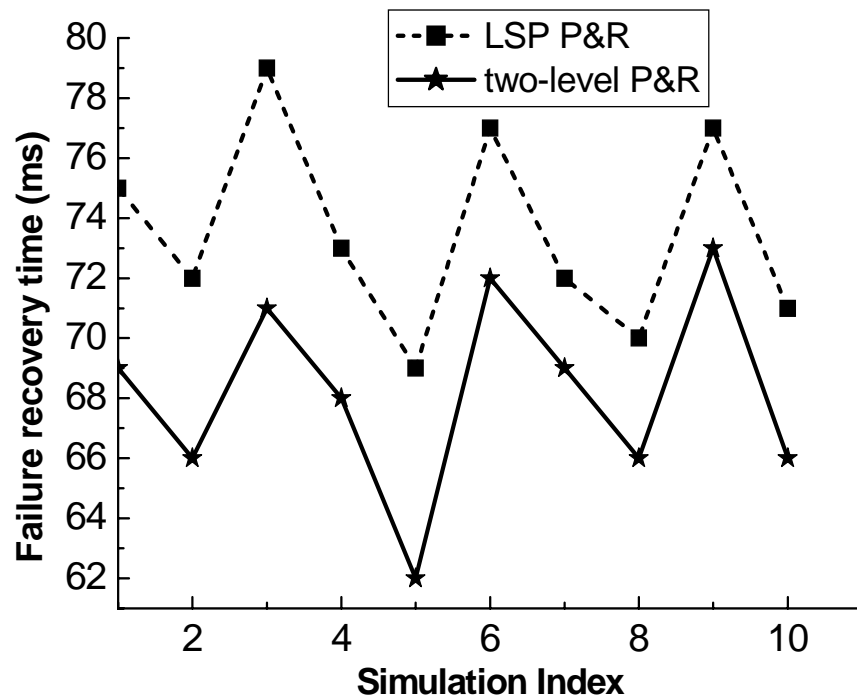
- Flexible and feasible P&R solutions which have faster failure recovery time and lower complexity.
- Efficient and scalable proposal for shared mesh restoration.
- Utilizing P&R mechanisms to provide mobility support in GMPLS-based networks.



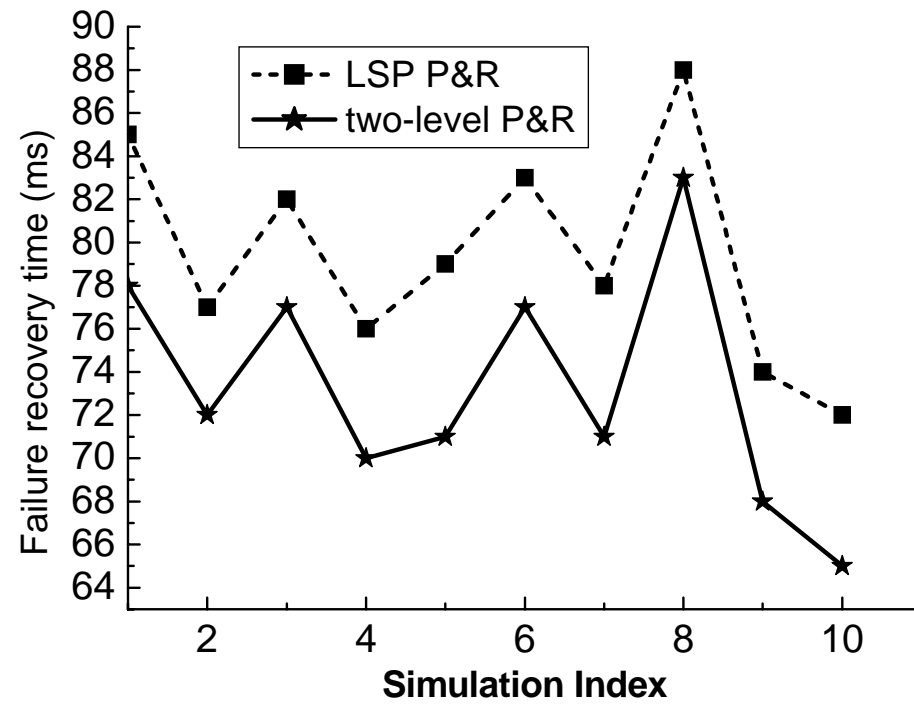
Research Results (I)

- An efficient two-level P&R scheme for GMPLS-based networks
 - LSP P&R is the first level. If a protection LSP, which is physically disjoint with selected working LSP, can not be found, LSP segment P&R will be applied as the second level.
 - An LSP segment selection algorithm is proposed to support our scheme.

Research Results (I)



(a) 18-node, 29-link network



(b) USANET



Research Results (I)

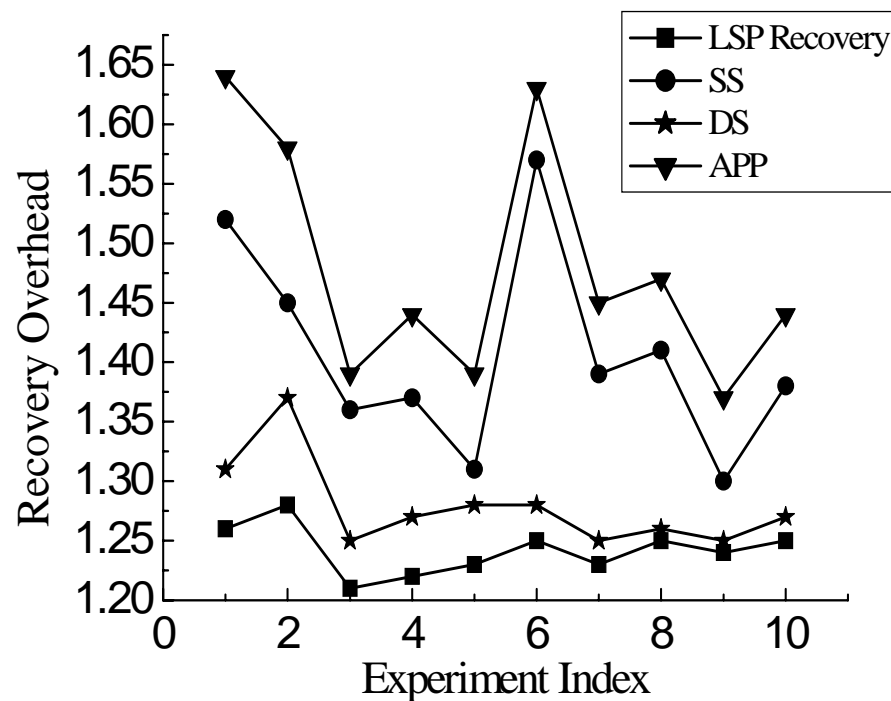
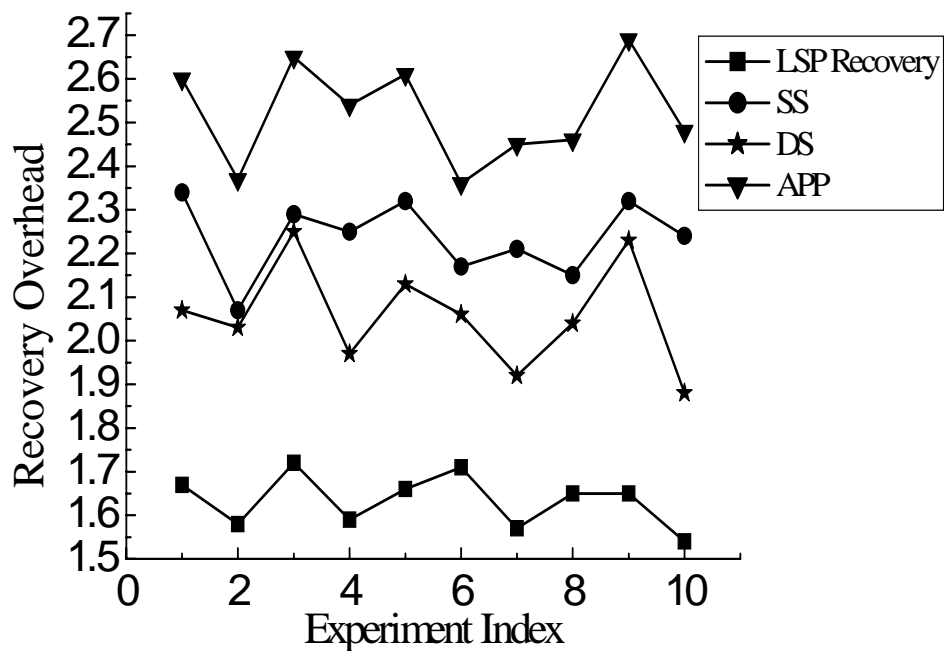
- Advantages
 - Higher protection path establishment acceptance rate.
 - Better Quality of Service (QoS) and reliability guarantees.
 - Shorter failure recovery time.



Research Results (II)

- Three novel overlapped LSP segment selection schemes are proposed.
 - The near-optimal set of overlapped LSP segments can be obtained by the proposed schemes, which have polynomial time complexity.
 - Differences among the proposed schemes are discussed and compared.

Research Results (II)





Research Results (II)

- Advantages
 - The near-optimal set of overlapped LSP segments can be obtained.
 - Complexity of LSP segment recovery design is much decreased.
 - Provisioning flexible choices for GMPLS-based P&R techniques according to different failure recovery time and resource utilization constraints.



Research Results (III)

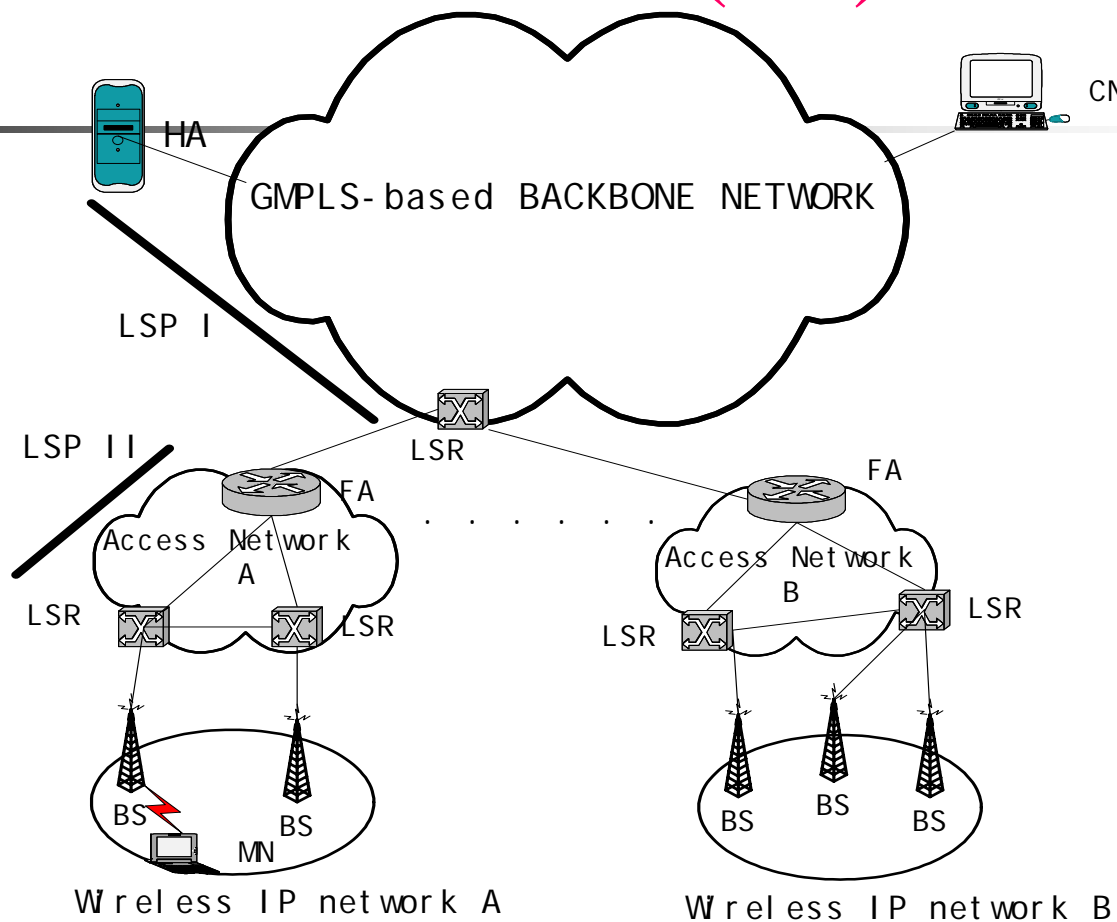
- Novel Disjoint-LSP Selection Scheme with SRLG in GMPLS-based Networks
 - It provides a common framework for conventional disjoint-path selection algorithms to find SRLG disjoint LSPs.
 - The proposed scheme has lower cost than that of others.



Research Results (IV)

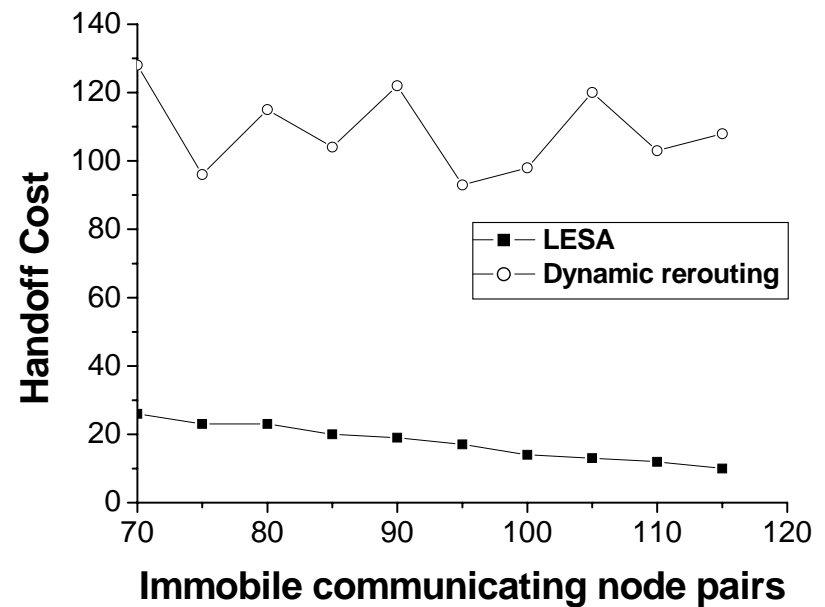
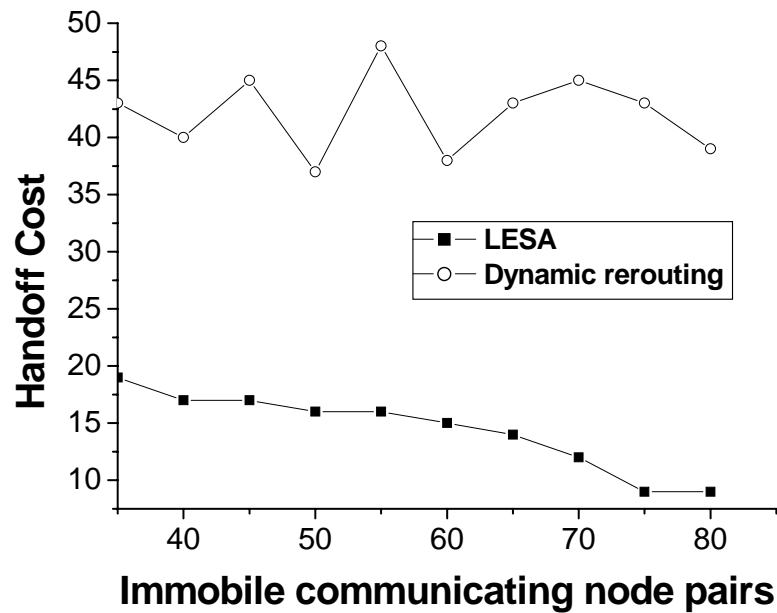
- GMPLS-based recovery scheme for fast handoff in mobile IP networks
 - Proposing GMPLS-based mobile IP network architecture.
 - Provisioning GMPLS with micro-mobility for the next-generation mobile broadband IP networks.
 - Improving resource utilization in GMPLS-based networks.

Research Results (IV)



- Architecture of integrating GMPLS and wireless IP network.

Research Results (IV)



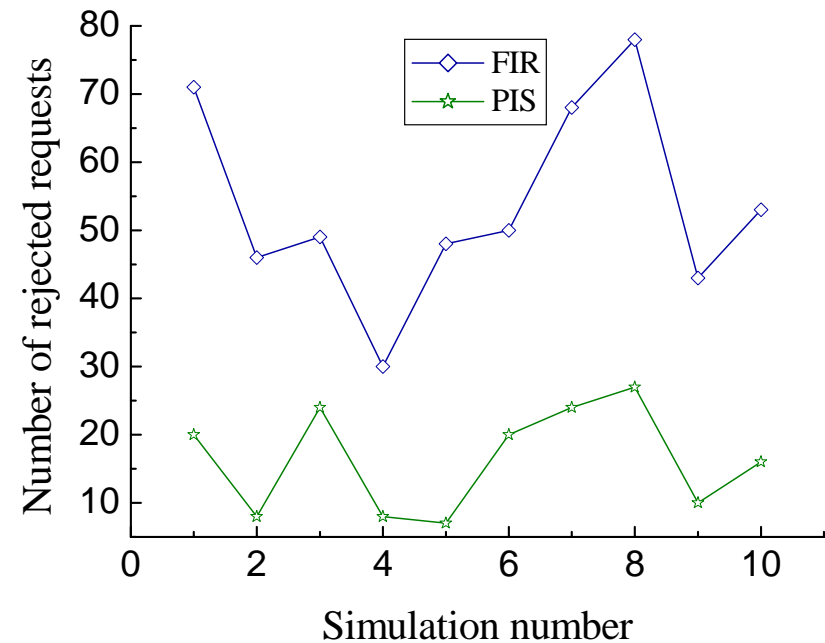
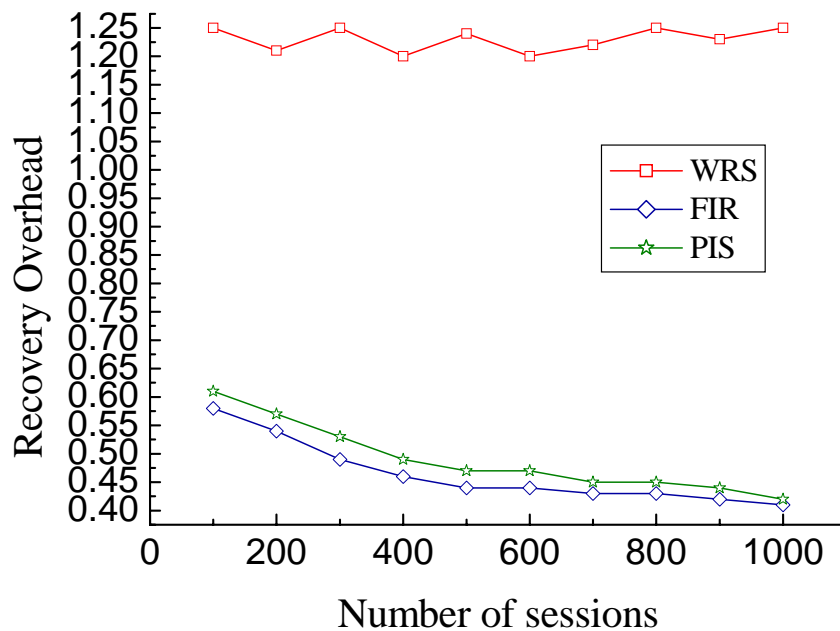
Simulation results



Research Results (V)

- Novel scheme for optimizing recovery resource sharing with traffic balancing
 - Minimum information is flooded in networks.
 - No additional signaling procedure is required.
 - Recovery resource sharing can be maximized.
 - Rejected connection setup requests are decreased significantly.

Research Results (V)



Simulation results



Research Results (VI)

- A framework for time guaranteed recovery in GMPLS-based networks
 - Recovering failure efficiently with the specific time constraint
 - Low design complexity
 - Resource sharing is utilized to improve the recovery overhead

A decorative graphic on the left side of the slide, consisting of a yellow square, a blue square, and a black crosshair.

PART IV

Design of MOEMS-based GMPLS-oriented Optical Switching System

A decorative graphic consisting of a yellow square and a blue square overlapping, with a black crosshair-like line passing through them.

Contents

- **Optical Switching**
- **2D MEMS-based Optical Switch for Optical Networking**



PART IV (1)

Optical Switching



Research Motivation (I)

- Optical switching technologies are very crucial for future mobile broadband all-optical IP networks.
- The continuous expanding networks demand large-port-count optical switches.
- Due to the difficulty in fabrication and control, few designs and architectures are suitable for building large optical switching matrix.



Research Motivation (II)

- Although optical MEMS-based switches as the most promising optical switch technology are commercially available now, the 2D crossbar architecture is not tractable for building large-port-count optical switches due to light beam divergence and the limitation of wafer fabrication.

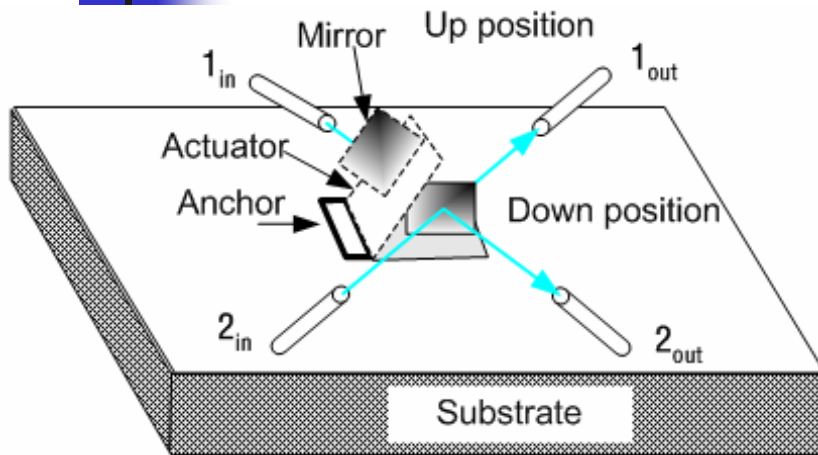


Research Goal

- To propose optical switching matrix designs suitable for building large 2D MEMS optical switches and achieving better performance in terms of beam divergence loss, mirror size, wafer size, port-to-port repeatability and power consumption.
- To propose switching architectures suitable for building large-port-count switching systems in GMPLS networks.

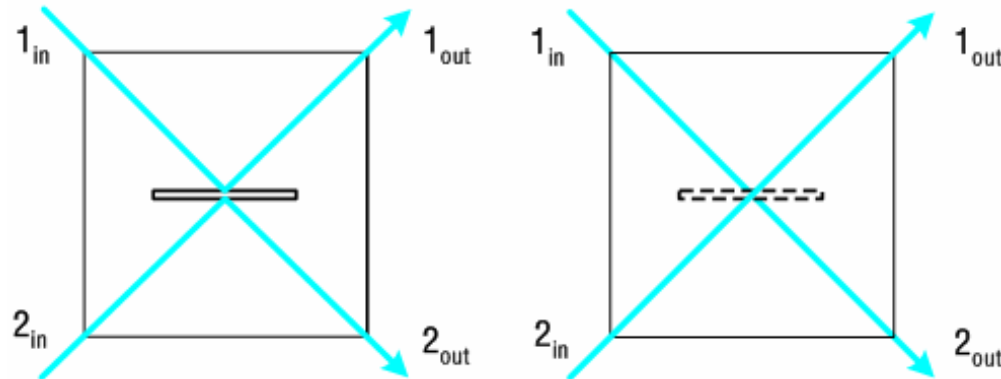
Research Results (I)

The simplest 2×2 MEMS-mirror switch module



(a) The 2×2 gap-closing MEMS switch example implemented based on the stress-bending and electrostatic.

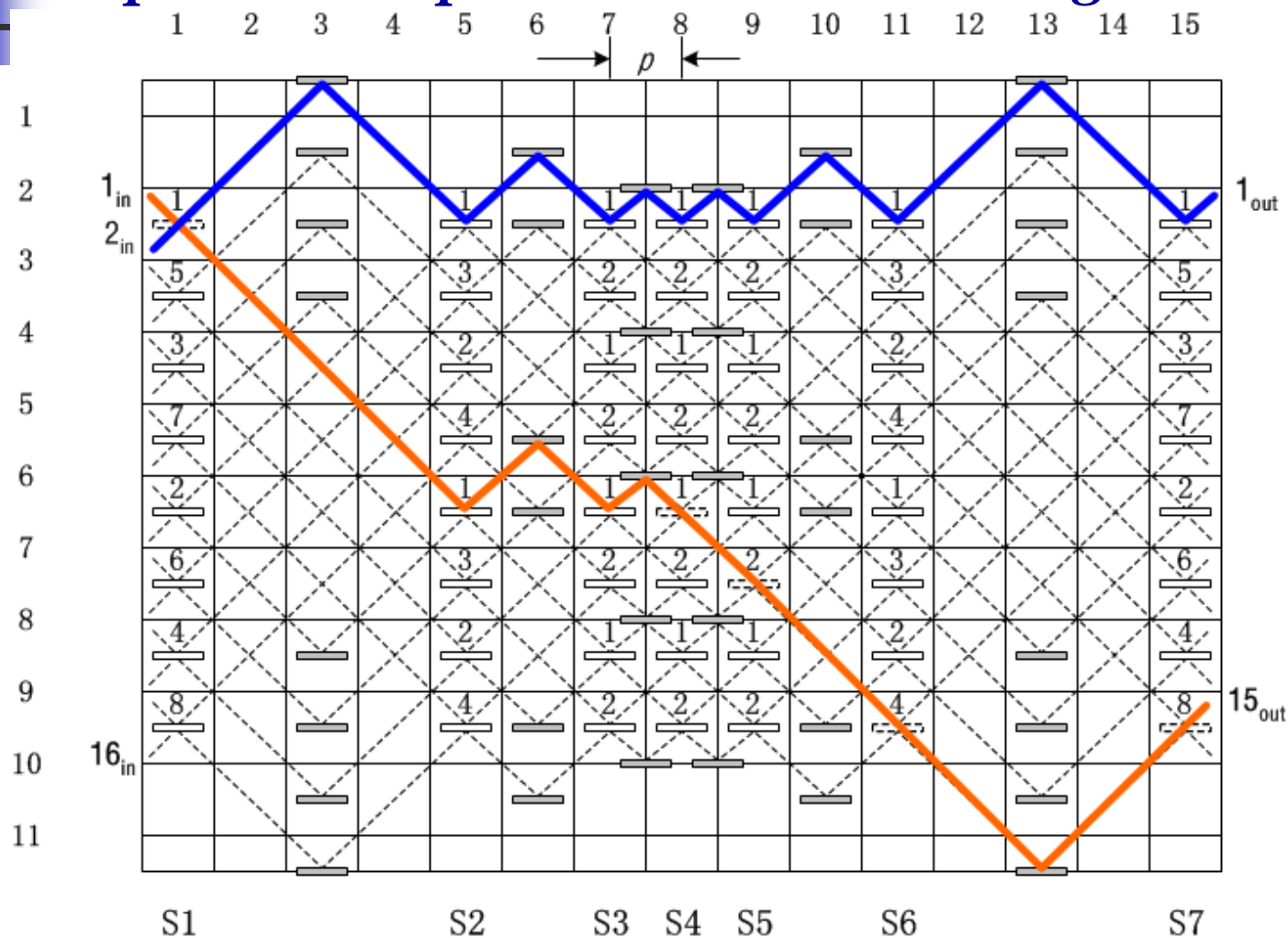
(b) Schematic platforms of (a).



The left diagram shows the optical paths when the double-sided mirror in DOWN position, and thus in the “Bar” state, while the right one corresponds to the mirror in UP position and thus the “Cross” state.

Research Results (I)

Proposed 2D optical MEMS switching matrix design





Research Results (I)

Advantages

over traditional 2D crossbar MEMS optical switch

- The required number of mirrors reduces from N^2 to $N(\log_2 N - 1/2)$ mirrors (N is the number of ports);
- superior optical power loss due to Gaussian beam divergence;
- better port-to-port repeatability performance;
- remarkably minifies the mirror radius and wafer area;
- and consequently the fabrication limit, tight requirements of actuation and servo control system are relaxed.

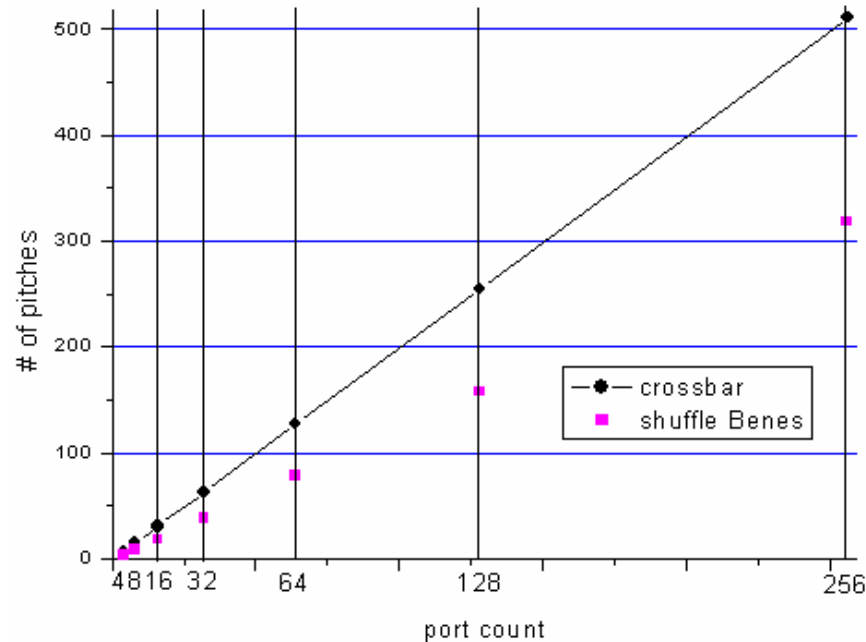
Research Results (I)

Comparison

- The path length

$$path\ length_{Shuffle\ Benes} = \sqrt{\left(\frac{3N}{4}p\right)^2 + \left(2p \sum_{k=0}^{\log_2 N - 2} 2^k\right)^2}$$

$$path\ length_{crossbar} = (2N - 1)p$$



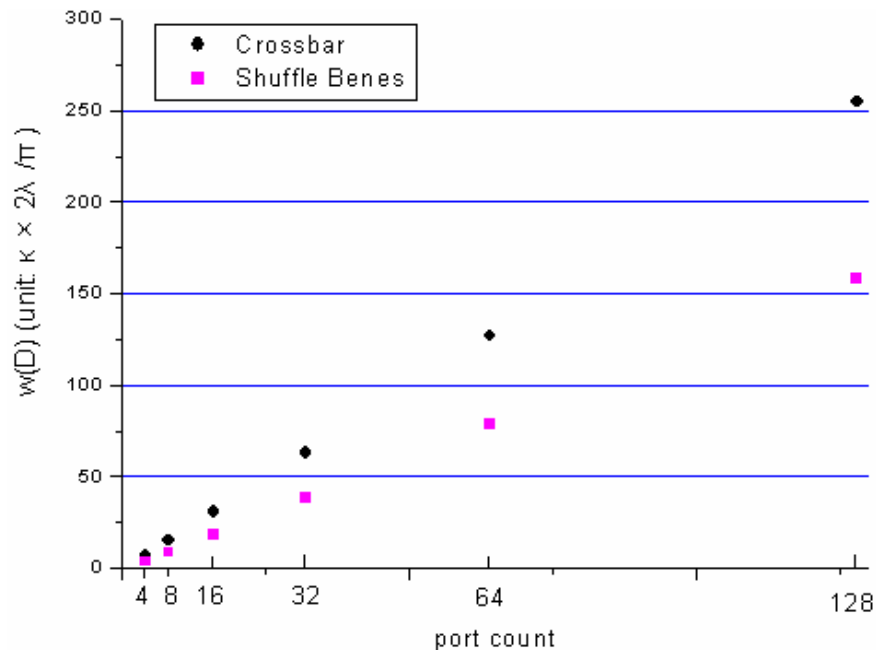
Research Results (I)

Comparison

■ Mirror size

$$w_{\text{shuffle Benes}}(D) = \frac{1}{2} \sqrt{\left(\frac{3N}{4}\right)^2 + \left(2^{\log_2 N - 2} \sum_{k=0}^{N-2} 2^k\right)^2} \kappa(2\lambda / \pi)$$

$$w_{\text{crossbar}}(D) = N \kappa(2\lambda / \pi)$$



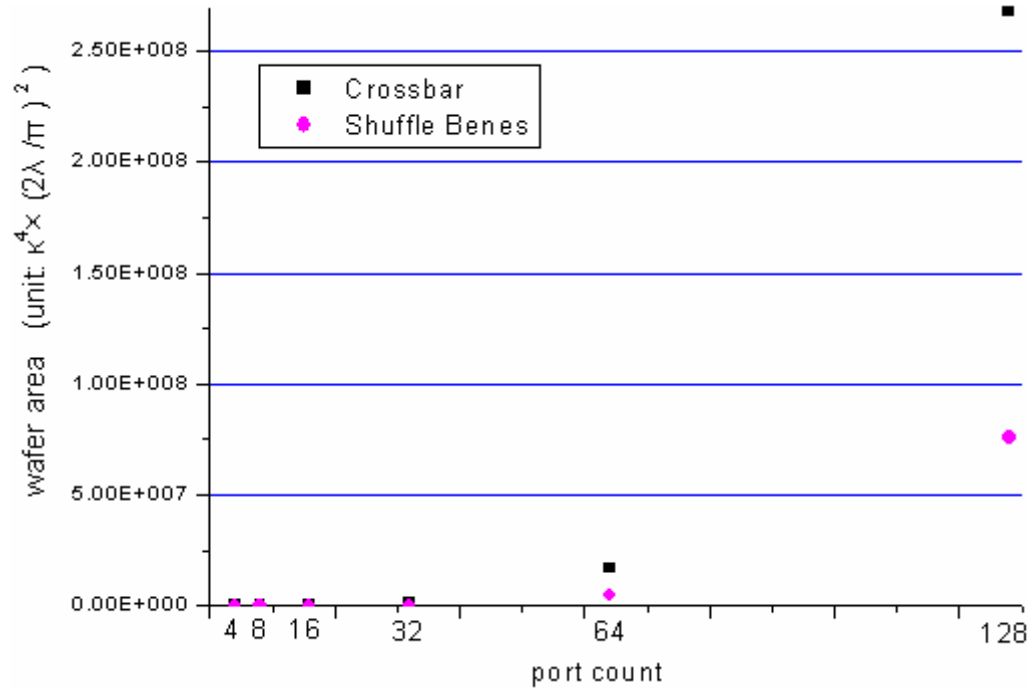
Research Results (I)

Comparison

■ Wafer size (switch dimension)

$$wafer\ size_{shuffle\ Benes} = \frac{1}{4} \left(\frac{3N}{4} \right) \cdot \left(2^{\sum_{k=0}^{\log_2 N-2} 2^k} \right) \cdot \left\{ \left(\frac{3N}{4} \right)^2 + \left(2^{\sum_{k=0}^{\log_2 N-2} 2^k} \right)^2 \right\} \kappa^4 (2\lambda / \pi)^2$$

$$wafer\ size_{crossbar} = D_{crossbar}^2 = N^4 \kappa^4 (2\lambda / \pi)^2$$





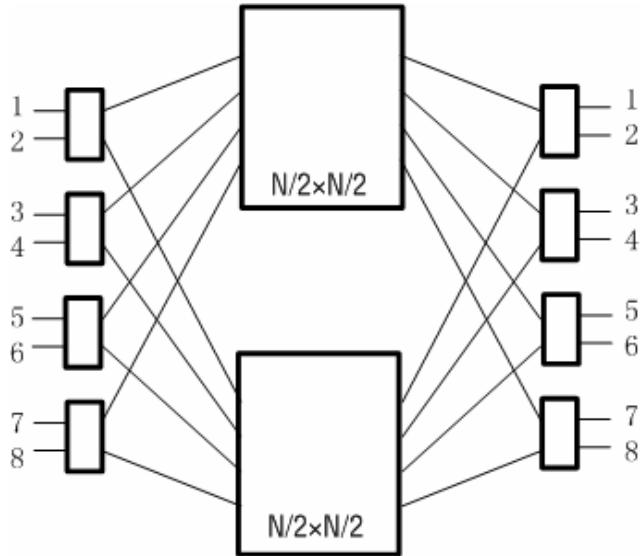
Research Results (I)

Disadvantages

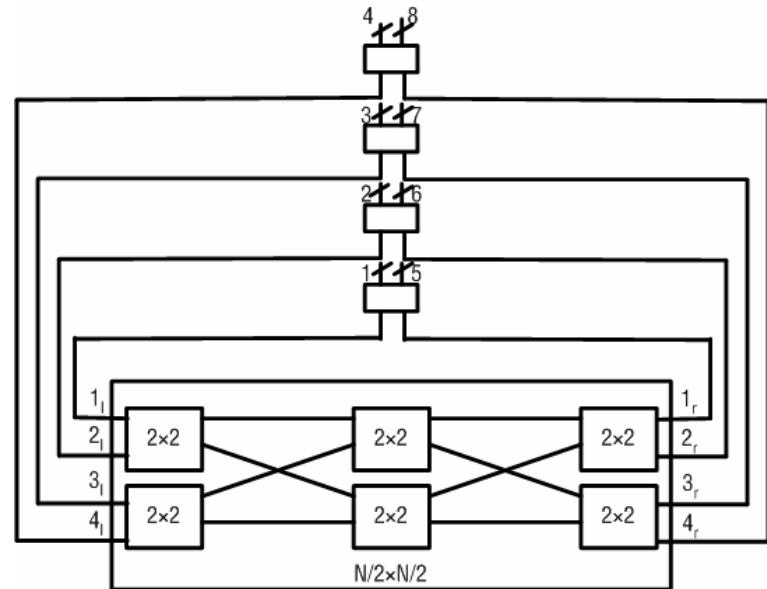
- Rearrangeable nonblocking;
- Control algorithms required to select routes.

Research Results (II)

Rearrangeably nonblocking OXC



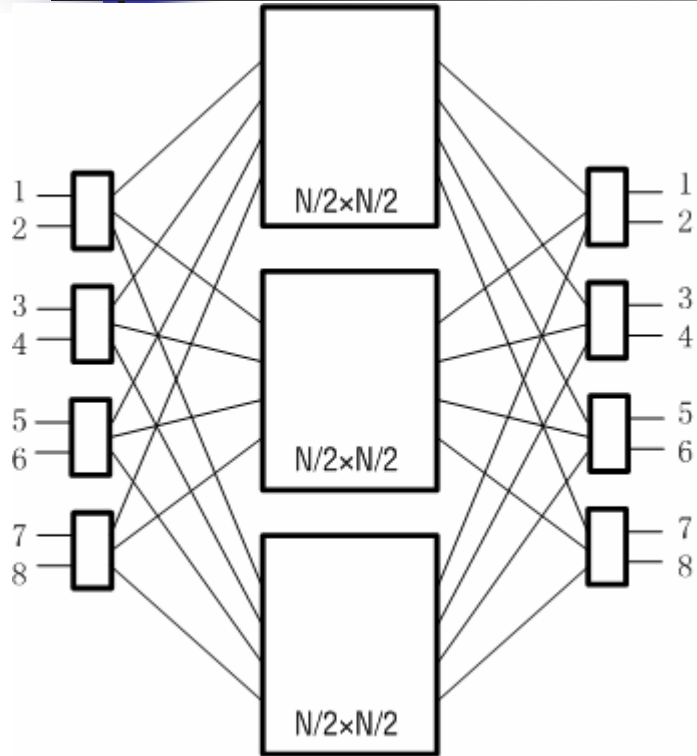
A. Traditional Benes architecture.



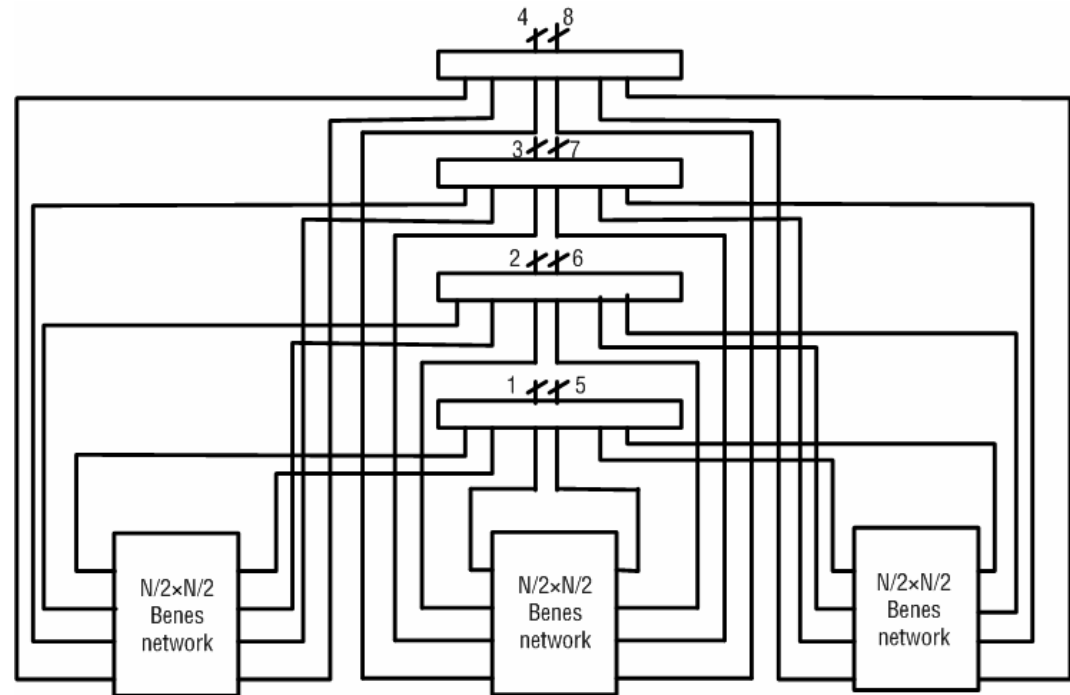
B. Bidirectional Benes architecture. Each line represents a bidirectional link. Subscripts l and r stand for left and right respectively.

Research Results (II)

Strictly nonblocking OXC



A. Traditional Benes architecture.



B. Bidirectional Benes architecture. Each line represents a bidirectional link. Subscripts l and r stand for left and right respectively.



Research Results (II)

Comparison

Rearrangeable:

- Rearrangeably nonblocking traditional architecture:

$$\begin{aligned} & N \quad 2 \times 2 \text{ switches} \\ & 2 \quad N/2 \times N/2 \text{ switches} \end{aligned}$$

- Rearrangeably nonblocking architecture we proposed:

$$\begin{aligned} & N/2 \quad 2 \times 2 \text{ switches} \\ & (N/4)[2\log_2(N/2)-1] \quad 2 \times 2 \text{ switches} \end{aligned}$$

Strict:

- Strictly nonblocking traditional architecture:

$$\begin{aligned} & N \quad 2 \times 3 \text{ switches} \\ & 3 \quad N/2 \times N/2 \text{ switches} \end{aligned}$$

- Strictly nonblocking architecture we proposed:

$$\begin{aligned} & (N/2) \times \log_2(N/2) \quad 2 \times 2 \text{ switches} \\ & \log_2(N/2) \times (N/4) \times [2\log_2(N/2)-1] \quad 2 \times 2 \text{ switches} \end{aligned}$$



PART IV (2)

2D MEMS-based Optical Switch for Optical Networking



Research Motivation (I)

- MEMS technology is used to fabricate optical switch. Many MEMS-based optical switches are actuated by high voltage, which makes it difficult to integrate the circuit and the mechanical part. It is necessary to find a method to lower the actuation voltage.



Research Motivation (II)

- There is the circuit in the MEMS design. Currently, the actuation voltage of a micro-mirror is not compatible with TTL or CMOS voltage, so a voltage conversion circuit is needed.

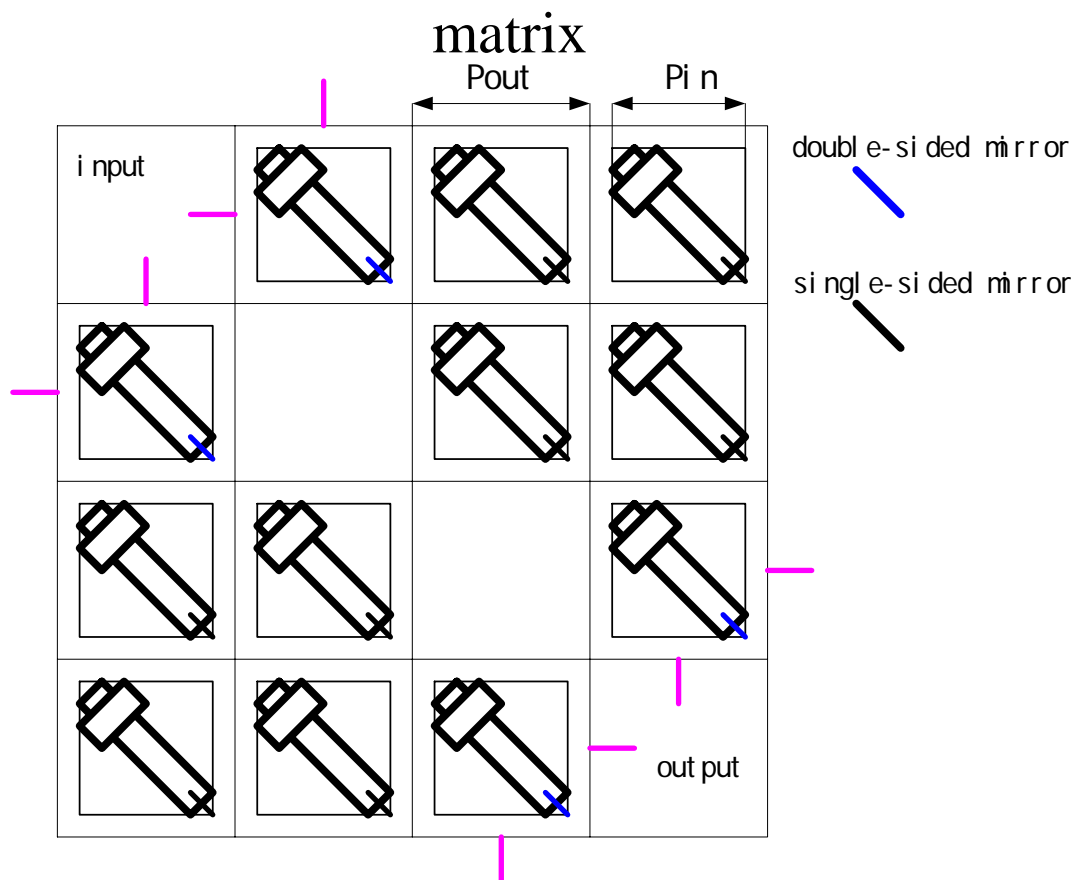


Research Goal

- Use CoventorWare to design micromirror with low actuation voltage.
- Looking for efficient approaches for voltage conversion.

Research Results (I)

Rearrangeable non-blocking Clos



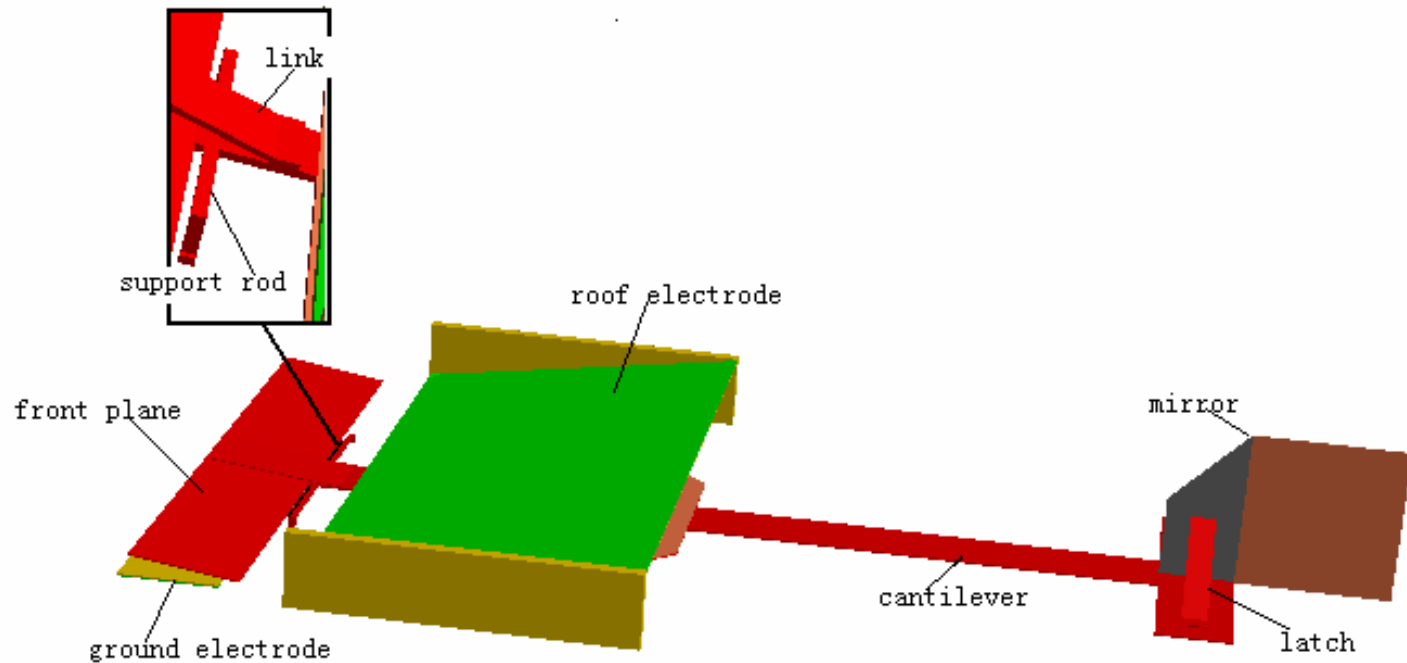


Research Results (I)

- Advantages
 - The number of the mirrors used is less than that in the conventional architecture.
 - All the light path lengths are the same in the novel architecture, so the insertion losses due to free-space distance have no difference among different input and output switching.
 - The maximum path length is less than that in the crossbar matrix.

Research Results (II)

- Micromirror structure



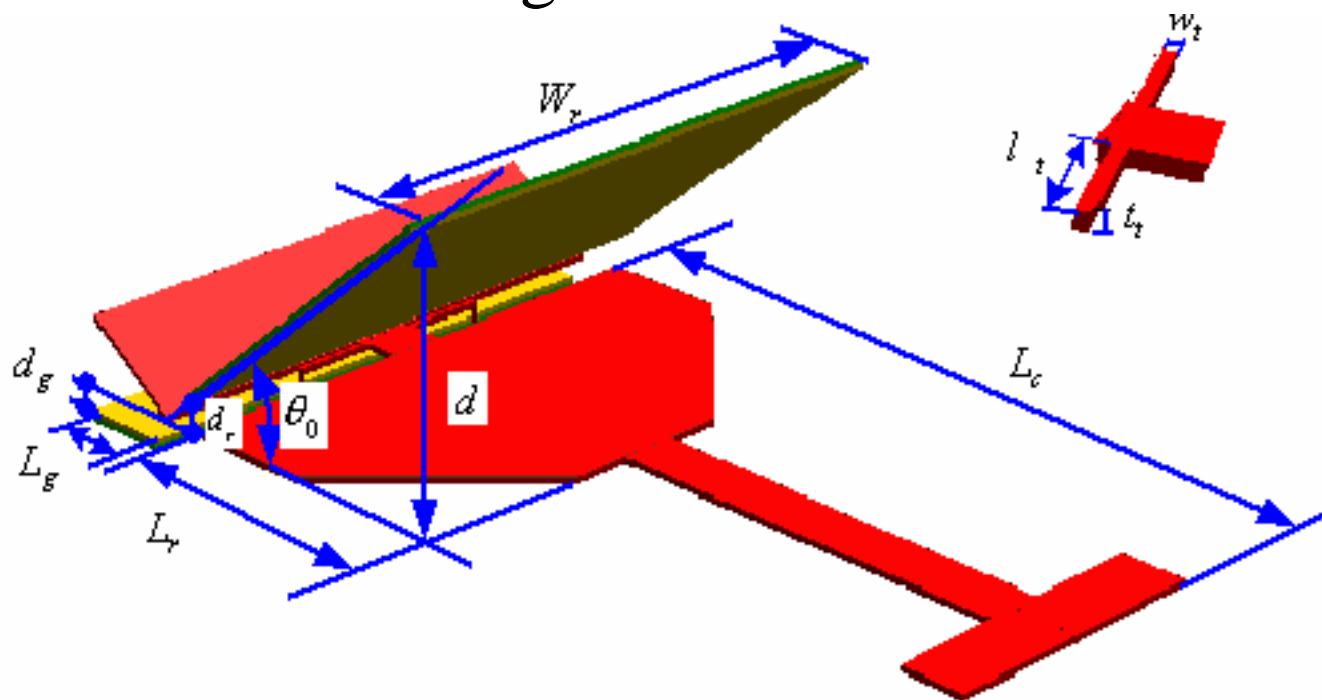
A decorative graphic consisting of a yellow square, a blue square, and a black crosshair.

Research Results (II)

- How to work
 - When a bias voltage is applied to the two electrodes, the cantilever rotates around the support rod until the cantilever touches the roof electrode. In this case, the switch is at OFF-state and the incident light beam propagates through the gap between the cantilever and the substrate.
 - When the bias voltage disappears, the cantilever rotates to the position that is parallel to the substrate, as a result of the restoring force on the support rod. Then, the switch is at ON-state, and the mirror reflects the incident light.

Research Results (II)

■ Parameter design

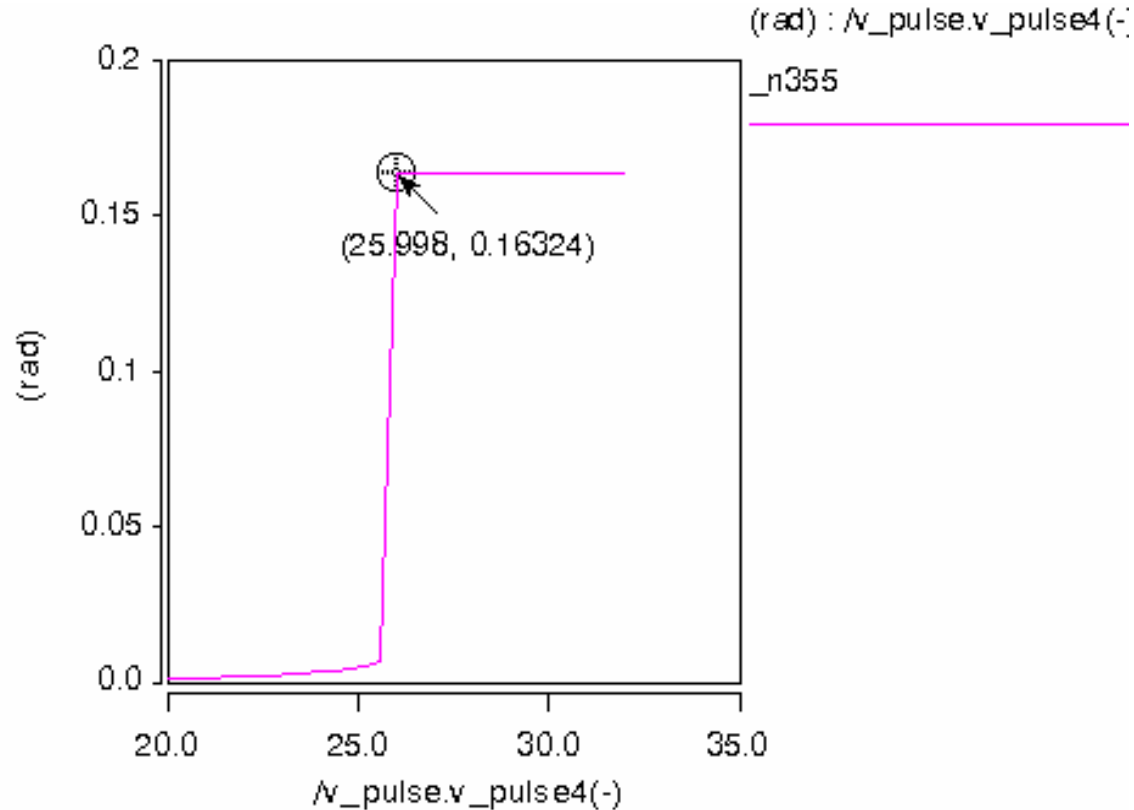


Research Results (II)

Design parameter	Value	Description
W_r	$400\mu m$	Width of roof electrode
L_r	$300\mu m$	Length of roof electrode
t_r	$1.2\mu m$	Thickness of cantilever and front plane
W_g	$500\mu m$	Width of ground electrode
L_g	$100\mu m$	Length of ground electrode
L_c	$740\mu m$	Length of cantilever
w_t	$5\mu m$	Width of support rod
l_t	$70\mu m$	Length of support rod
t_t	$1.2\mu m$	Thickness of support rod
d	$50\mu m$	Separation between highest point of tilt roof electrode and cantilever
d_r	$2\mu m$	Separation between lowest point of tilt roof electrode and cantilever
d_g	$2\mu m$	Separation between cantilever and the ground electrode
S	$120\mu m$	Length of one side of mirror
θ_0	9.5°	Initial angle of tilt roof electrode

Research Results (II)

- Pull-in voltage





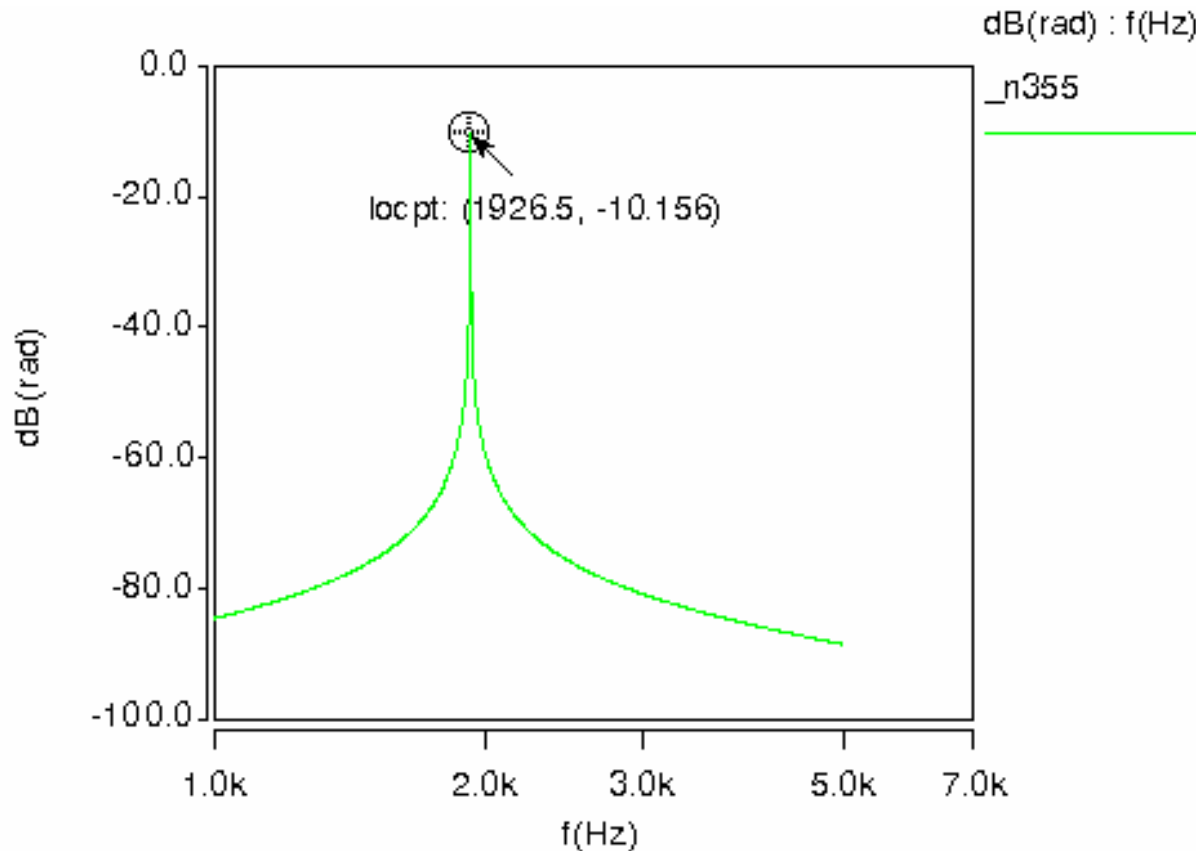
Research Results (II)

- Pull-in voltage
 - When the applied voltage is lower than 26V, the tilt angle is linear with the applied voltage.
 - When the applied voltage is higher than 26V, the tilt angle reaches the maximum value.

The Pull-in voltage is 26V, and that is the minimum actuation voltage.

Research Results (II)

- Resonant frequency





Research Results (II)

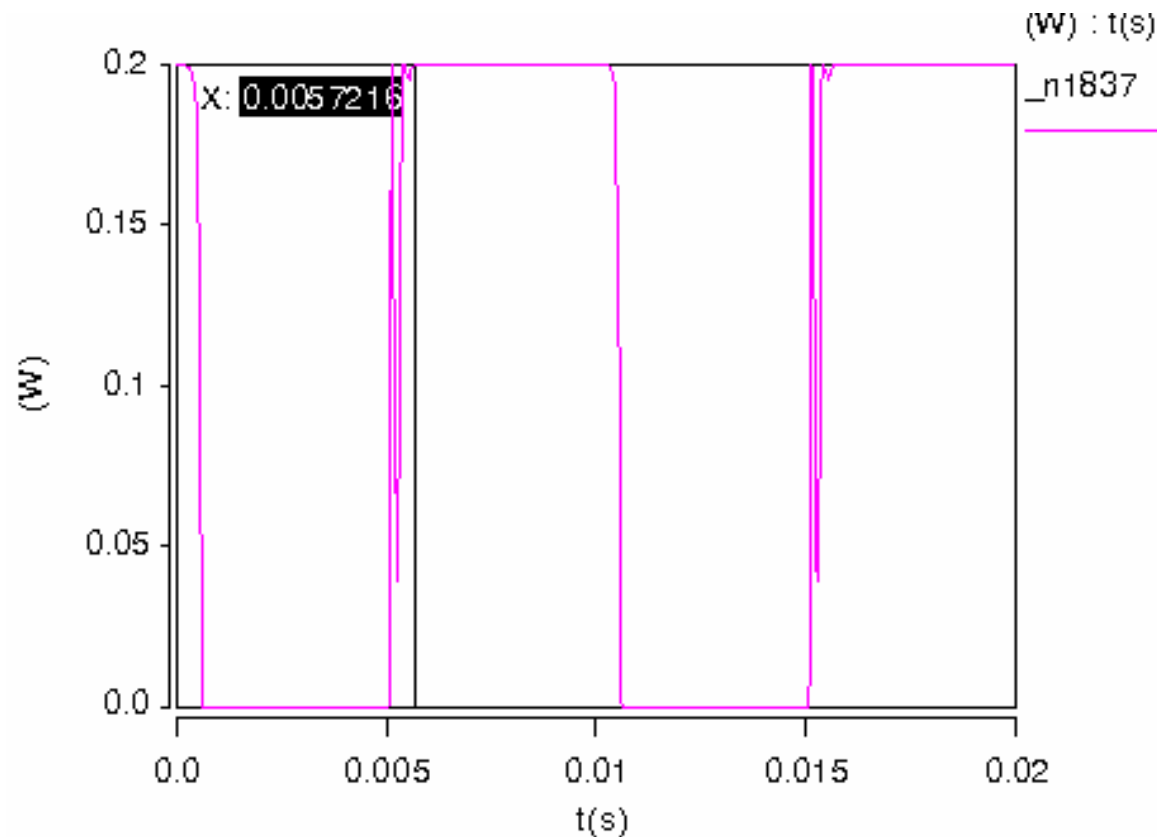
- Resonant frequency

The resonant frequency is 1.9kHz.

The resonant frequency of the micromirror is high enough to protect it from disturbance.

Research Results (II)

- Simulation result

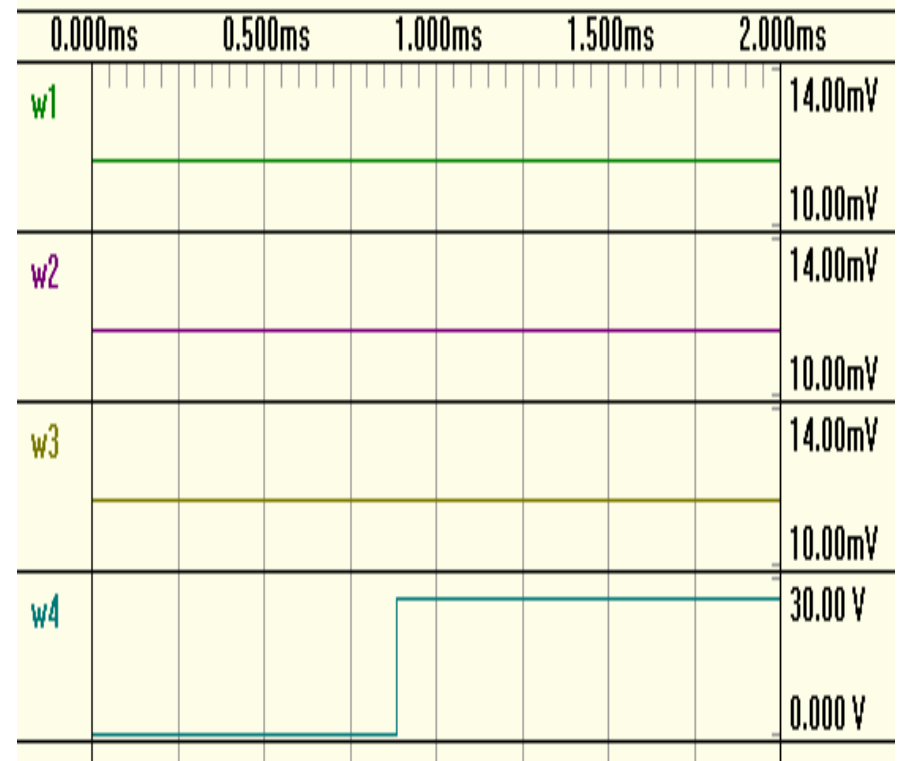
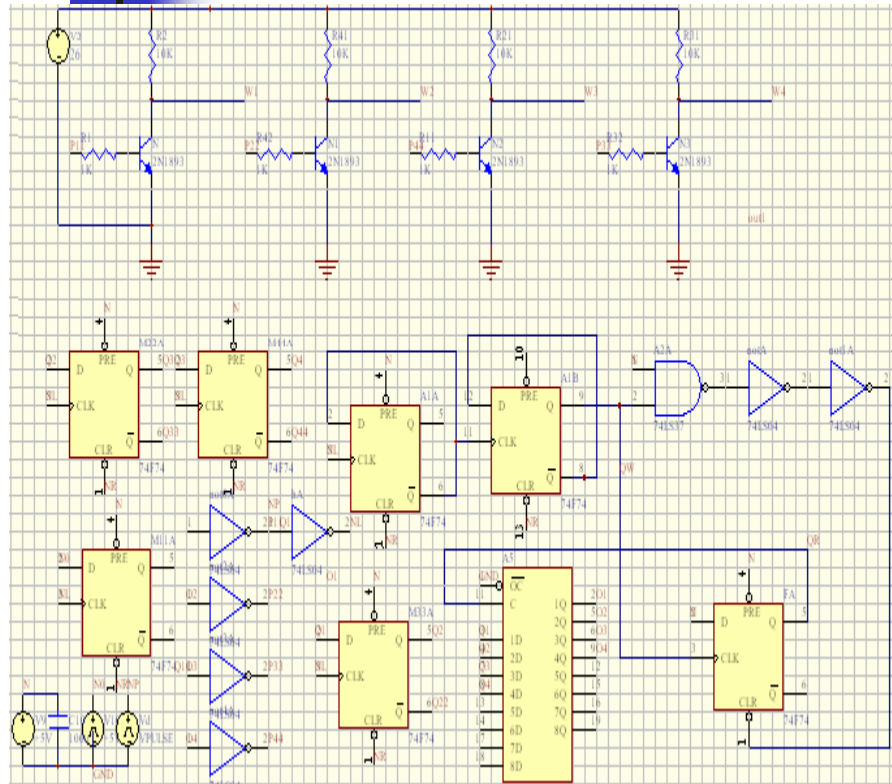




Research Results (II)

- Advantages
 - The use of the tilt roof electrode lowers the actuation voltage and prevents the vibration of the cantilever.
 - The micromirror is designed, according to the Clos matrix. This novel switching architecture makes the micromirror size and required tilt angle smaller.

Research Results (III)



The schematic diagram of control circuit.

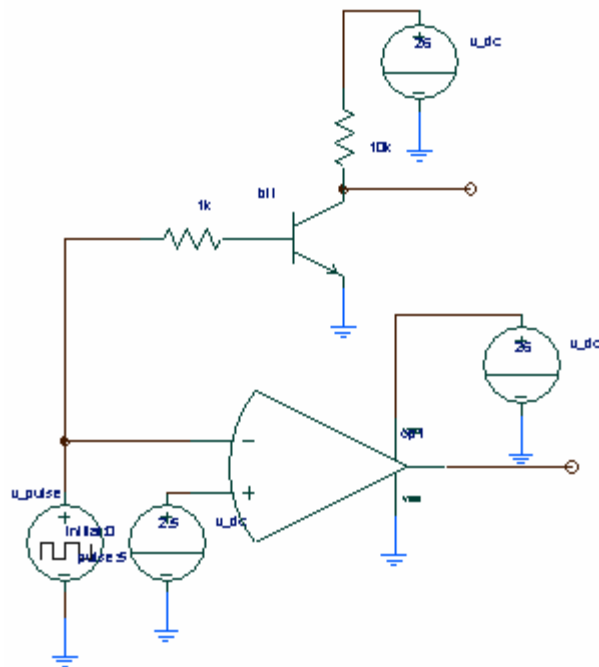
The simulation result



Research Results (III)

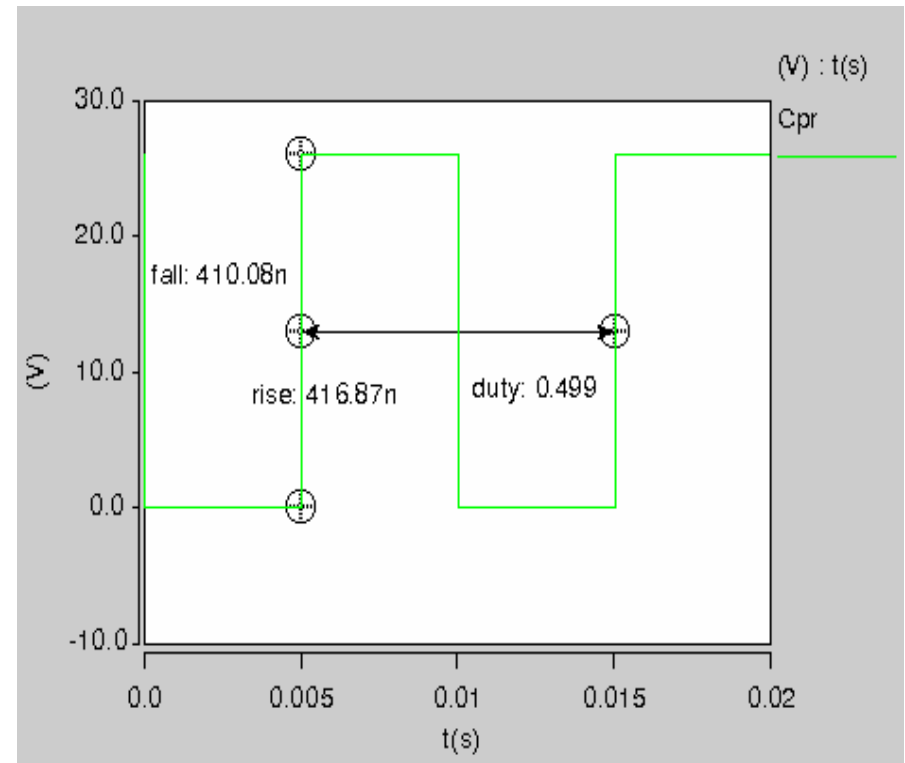
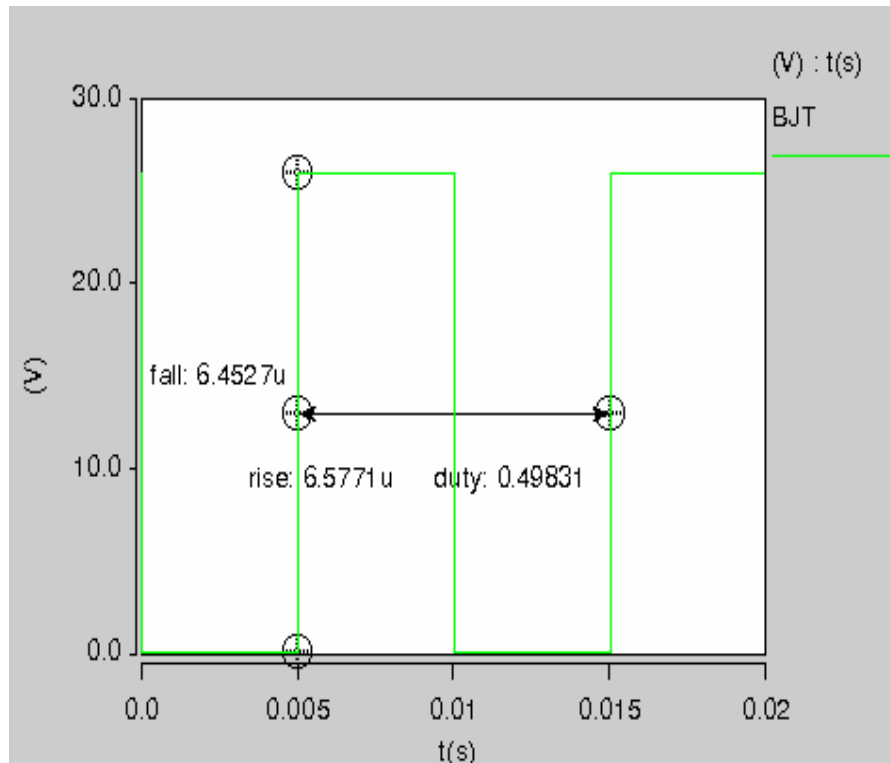
- The schematic diagram shows the control circuit of 4 micro-mirrors in a 4×4 crossbar matrix.
- The input address is 0001.

Research Results (IV)



- This schematic diagram intends to compare the performance of a BJT and a comparator as a voltage converter respectively.

Research Results (IV)

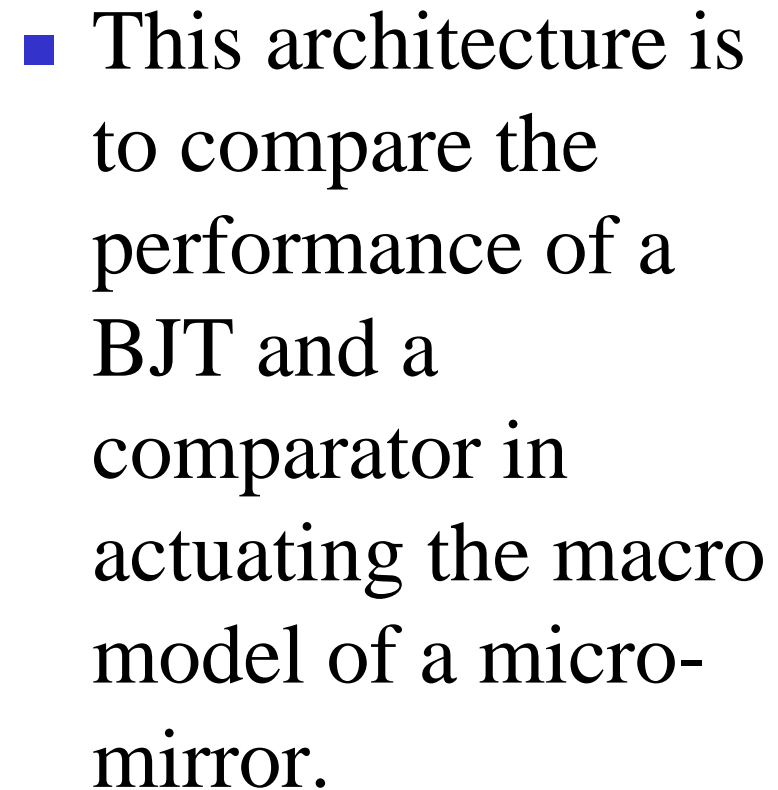


The simulation results

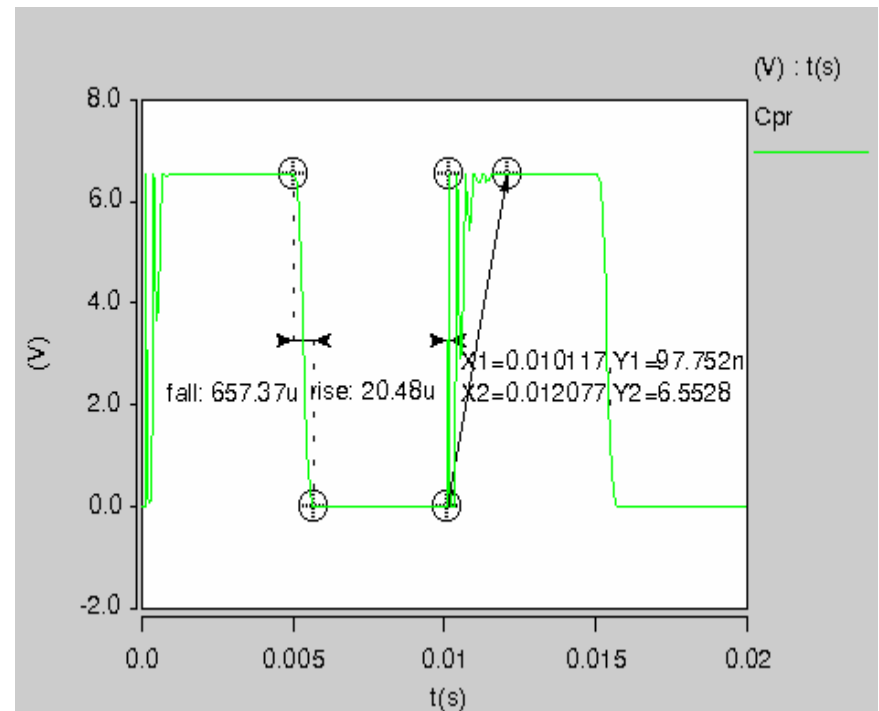
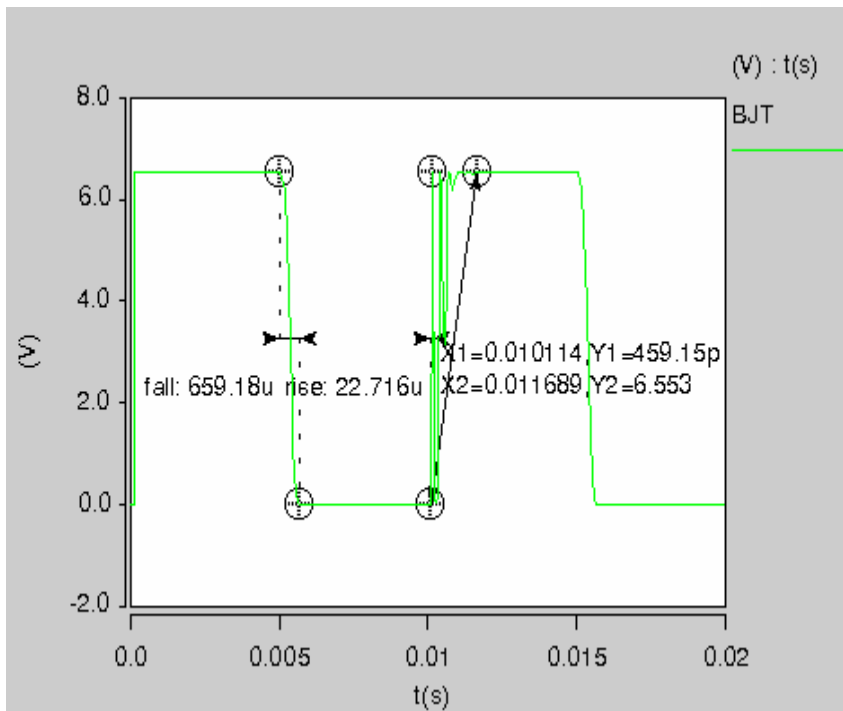


Research Results (IV)

- The comparator improves the performance obviously as a voltage converter compared to the BJT in fall time, rise time and duty circle for comparisons.



Research Results (V)



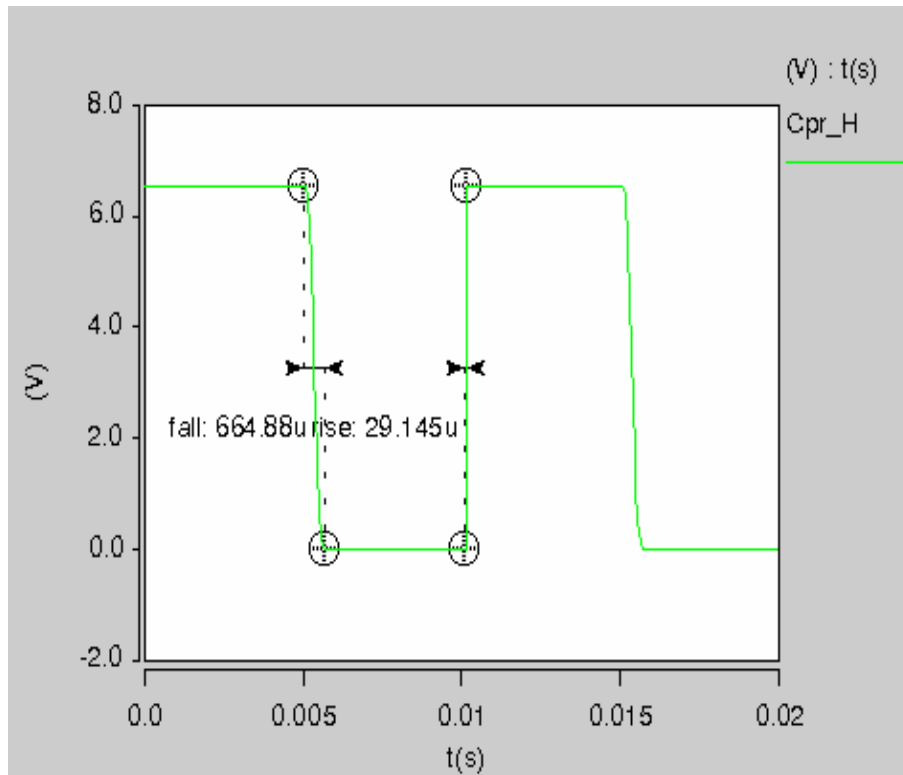
The simulation results



Research Results (V)

- From the simulation result, we obtain that the comparator improves the switching performance a little.

Research Results (V)



- This result is simulated by a hysteretic comparator as a voltage converter to actuate the macro model.
- It is obvious that the switching performance is improved greatly.